

# Propagation of Syndesmotic Injuries During Forced External Rotation in Flexed Cadaveric Ankles

Alexander Ritz Mait,<sup>\*†</sup> MS, Jason Lee Forman,<sup>†</sup> PhD, Bingbing Nie,<sup>†</sup> PhD, John Paul Donlon,<sup>†</sup> BS, Adwait Mane,<sup>†</sup> MS, Ali Reza Forghani,<sup>†</sup> PhD, Robert B. Anderson,<sup>‡</sup> MD, M. Truitt Cooper,<sup>§</sup> MD, and Richard W. Kent,<sup>†</sup> PhD

*Investigation performed at the Center for Applied Biomechanics, University of Virginia, Charlottesville, Virginia, USA*

**Background:** Forced external rotation of the foot is a mechanism of ankle injuries. Clinical observations include combinations of ligament and osseous injuries, with unclear links between causation and injury patterns. By observing the propagation sequence of ankle injuries during controlled experiments, insight necessary to understand risk factors and potential mitigation measures may be gained.

**Hypothesis:** Ankle flexion will alter the propagation sequence of ankle injuries during forced external rotation of the foot.

**Study Design:** Controlled laboratory study.

**Methods:** Matched-pair lower limbs from 9 male cadaveric specimens (mean age,  $47.0 \pm 11.3$  years; mean height,  $178.1 \pm 5.9$  cm; mean weight,  $94.4 \pm 30.9$  kg) were disarticulated at the knee. Specimens were mounted in a test device with the proximal tibia fixed, the fibula unconstrained, and foot translation permitted. After adjusting the initial ankle position (neutral,  $n = 9$ ; dorsiflexed,  $n = 4$ ; plantar flexed,  $n = 4$ ) and applying a compressive preload to the tibia, external rotation was applied by rotating the tibia internally while either lubricated anteromedial and posterolateral plates or calcaneal fixation constrained foot rotation. The timing of osteoligamentous injuries was determined from acoustic sensors, strain gauges, force/moment readings, and 3-dimensional bony kinematics. Posttest necropsies were performed to document injury patterns.

**Results:** A syndesmotic injury was observed in 5 of 9 (56%) specimens tested in a neutral initial posture, in 100% of the dorsiflexed specimens, and in none of the plantar flexed specimens. Superficial deltoid injuries were observed in all test modes.

**Conclusion:** Plantar flexion decreased and dorsiflexion increased the incidence of syndesmotic injuries compared with neutral matched-pair ankles. Injury propagation was not identical in all ankles that sustained a syndesmotic injury, but a characteristic sequence initiated with injuries to the medial ligaments, particularly the superficial deltoid, followed by the propagation of injuries to either the syndesmotic or lateral ligaments (depending on ankle flexion), and finally to the interosseous membrane or the fibula.

**Clinical Relevance:** Superficial deltoid injuries may occur in any case of hyper-external rotation of the foot. A syndesmotic ankle injury is often concomitant with a superficial deltoid injury; however, based on the research detailed herein, a deep deltoid injury is then concomitant with a syndesmotic injury or offloads the syndesmosis altogether. A syndesmotic ankle injury more often occurs when external rotation is applied to a neutral or dorsiflexed ankle. Plantar flexion may shift the injury to other ankle ligaments, specifically lateral ligaments.

**Keywords:** syndesmosis; tibiofibular; ligament; injury sequence; nonsenescent cadaveric specimens; ankle flexion

Human ankles are complicated mechanical structures featuring 2 main joints: the talocrural joint, which articulates between the tibia, fibula, and talus, and the subtalar joint, which articulates between the talus and calcaneus.<sup>4,11,13,23</sup> Ligaments constrain these joints and their associated bones but permit physiological ranges of motion.<sup>5,22,23</sup> Commonly

in athletics, injuries to the ankle joint occur to the lateral structures of the anterior talofibular ligament (ATaFL), calcaneofibular ligament (CFL), and posterior talofibular ligament (PTaFL) because of severe inversion of the foot.<sup>1,7,11,34</sup> Less common are injuries to the tibiofibular syndesmosis, occurring in less than 20% of all ankle sprains.<sup>1,2,6,9,14,23,33</sup>

Despite a lower occurrence rate compared with lateral ankle sprains, syndesmotic ankle sprains are accompanied by a lengthy recovery time.<sup>1,3,8,10,14,23,29,33</sup> American

The Orthopaedic Journal of Sports Medicine, 6(6), 2325967118781333  
DOI: 10.1177/2325967118781333  
© The Author(s) 2018

This open-access article is published and distributed under the Creative Commons Attribution - NonCommercial - No Derivatives License (<http://creativecommons.org/licenses/by-nc-nd/4.0/>), which permits the noncommercial use, distribution, and reproduction of the article in any medium, provided the original author and source are credited. You may not alter, transform, or build upon this article without the permission of the Author(s). For reprints and permission queries, please visit SAGE's website at <http://www.sagepub.com/journalsPermissions.nav>.

football is a widely cited contact sport for syndesmotic ankle injuries. Over a 5-year span, professional American football players had an average, per player, time loss of 2.5 weeks, 11.7 practices, and 1.4 games from syndesmotic ankle sprains compared with 1.25 weeks, 3.5 practices, and 0.3 games from lateral ankle sprains, respectively.<sup>8,33</sup> Syndesmotic ankle sprains, where recovery time can exceed 31 days, are often highly debilitating injuries in which athletes have trouble performing moves (eg, cutting and pushing off) and experience chronic pain.<sup>1,11,23,28,29,33</sup> Often, proper diagnoses and treatment of syndesmotic ankle sprains are challenging.<sup>10,33</sup>

External rotation is often hypothesized as the key mechanism of syndesmotic ankle injuries.<sup>1,2,8,14,23,29,31-34</sup> External rotation of the foot is believed to cause the talus to wedge between the tibia and fibula, which generates tibiofibular diastasis.<sup>14,33</sup> This diastasis increases the risk of ruptures to the anterior and posterior tibiofibular ligaments (ATiFL and PTiFL) with possible propagation to the interosseous membrane (IOM).<sup>1-4,14,34</sup> With such damaging consequences and extended recovery time, understanding the mechanics of syndesmotic ankle sprains is necessary to inform future clinical care and prevention.

The sequence and propagation of injuries among the ankle ligaments during external rotation of the foot, and their sensitivity to ankle orientation in the other planes of motion, remain unclear. Previous studies identified injuries in posttest dissections with no means to determine the sequence of injuries.<sup>18,19,31,32</sup> By observing the sequence of injuries, the propagation of injuries through the structures of the ankle may be understood, thus informing efforts for injury prediction (eg, by understanding the ligament that is the first to be injured), modeling, and prevention. Understanding the propagation sequence may also inform diagnosis efforts by providing information on potential concomitant injury indicators.

The objectives of this study were to generate ankle injuries in cadaveric specimens via external rotation, using realistic proximal and distal boundary conditions, to determine the patterns and sequences of injuries that occur and to evaluate how initial dorsiflexion and plantar flexion modify the pattern and sequence of injuries. From these objectives, it was hypothesized that ankle flexion will alter the incidence of syndesmotic injuries and the sequence of ankle injuries during forced external rotation. These results are anticipated to have relevance in both clinical and biomechanical research<sup>20,21</sup> settings.

## METHODS

### Specimen Preparation

Experiments were conducted on the right and left lower limbs from 9 fresh-frozen male cadaveric specimens (Table 1). Specimens were tested in 3 subsamples denoted by the initial flexion position, with 9 left legs tested in neutral, 4 right legs tested in dorsiflexion, and 4 right legs tested in plantar flexion. The legs tested in plantar flexion and dorsiflexion were the matched pairs to those tested in neutral, with a matched-pair right leg not tested for 1 neutral leg (Table 1). Nonsenescent cadaveric limbs were acquired for testing with the intention of targeting the mean height, weight, and age of professional American football players.<sup>17</sup> Although the target height and weight of professional American football players were not met completely in this study (Table 1), the current study tested cadaveric specimens of the largest size and youngest age at death compared with previous studies,<sup>18,19,31</sup> thus approaching professional player anthropometry more closely than other cadaveric specimens studied in the literature. All specimens were acquired with the approval of the university's institutional review board and were prepared in accordance with its procedures and policies. The specimens were procured from various donor procurement organizations possessing necessary serology reports and consent forms. Before testing, all limbs were confirmed free of blood-borne pathogens. Computed tomography (CT) was performed to confirm the absence of bony trauma. All limbs were stored at  $-15^{\circ}\text{C}$  and thawed to room temperature 48 hours before test preparation.

To prepare the specimens for testing, the tibia and fibula were disarticulated at the knee. The medial and lateral intercondylar eminences were shaved off to flatten the tibial plateau. Soft tissue was removed from the tibial plateau and the medial, anterior, and posterior aspects of the tibial shank approximately 10 cm distal to the tibial plateau. Care was taken to not disturb the proximal tibiofibular ligaments and IOM. The superficial tissue around the fibula was also left in place. The proximal tibia was rigidly attached to a potting cup at the center of the tibial plateau (Figure 1A) with the fibula left unconstrained.<sup>16</sup> Wood screws were drilled into the tibial plateau and around the medial aspect of the tibial shank at varying heights and angles. For increased rigidity, threaded rods were drilled from anterior to posterior through the proximal tibia and

\*Address correspondence to Alexander Ritz Mait, MS, Center for Applied Biomechanics, University of Virginia, 4040 Lewis and Clark Drive, Charlottesville, VA 22911, USA (email: arm7sb@virginia.edu).

†Center for Applied Biomechanics, University of Virginia, Charlottesville, Virginia, USA.

‡OrthoCarolina, Charlotte, North Carolina, USA.

§Department of Orthopaedic Surgery, University of Virginia, Charlottesville, Virginia, USA.

One or more of the authors has declared the following potential conflict of interest or source of funding: Funding for this study was provided by Biocore and the Foot and Ankle Subcommittee of the National Football League. R.B.A. has received royalties from Wright Medical Technology, Arthrex, Zimmer Biomet, and DJO; has received educational support from Wright Medical Technology, Arthrex, Pacira Pharmaceuticals, and Bioventus; is a consultant for Wright Medical Technology, Arthrex, Zimmer Biomet, Amniox Medical, DJO, and Olympus Biotech; is a paid speaker/presenter for Wright Medical Technology, Arthrex, Pacira Pharmaceuticals, and Bioventus; and has received hospitality payments from Wright Medical Technology, Zimmer Biomet, Amniox Medical, DJO, the Musculoskeletal Transplant Foundation, Pacira Pharmaceuticals, Bioventus, and Olympus Biotech. M.T.C. has received hospitality payments from Small Bone Innovations and Treace Medical Concepts and is a consultant for Treace Medical Concepts. R.W.K. has ownership interests in Biocore, one of the study sponsors.

Ethical approval for this study was obtained from the University of Virginia Institutional Review Board for Human Surrogate Use (No. CAB2014-07).

TABLE 1  
Whole-Body Specimen Anthropometry and Test Input Loading Conditions

Run No. <sup>a</sup>	Specimen No. <sup>b</sup>	Sex	Age, y	Height, cm	Weight, kg	Preload, kN	Input Rotation Magnitude, deg
1	696R	Male	49	175.3	61.2	2	60
2, 10	680L, R	Male	58	175.3	63.0	2	53, 90
3, 14	682L, R	Male	54	183.0	57.1	2	60, 90
4, 12	615L, R	Male	57	183.0	94.3	2	90, 90
5, 13	794L, R	Male	57	177.8	149.2	2	90, 90
6, 17	801L, R	Male	36	173.0	92.0	2	90, 90
7, 11	612L, R	Male	36	167.5	113.4	2	90, 90
8, 15	752L, R	Male	27	182.9	97.1	2	90, 90
9, 16	757L, R	Male	49	185.4	122.0	2	90, 90
Mean, 9 specimens			47	178.1	94.4		
National Football League mean <sup>17</sup>			27	188.1	113.6		

<sup>a</sup>Specimens in runs 1 to 9 were neutral (n = 9), runs 10 to 13 were plantar flexed (n = 4), and runs 14 to 17 were dorsiflexed (n = 4).

<sup>b</sup>"L" indicates the left lower limb specimen, tested first, and "R" indicates the matched-pair right lower limb specimen, tested second.

sunk into a plastic insert on the posterior side of the potting cup. To complete the connection between the tibia and the potting cup, Bondo body filler (part #261; 3M) was placed in the cup surrounding the tibial plateau.

To assist in identifying the timing of injuries, triaxial rosette strain gauges (Micro-Measurements; Vishay Precision Group) were attached to both the tibia and fibula for select specimens (Figure 1B). Strain gauges were affixed to the specimens such that the second (middle) gauge was approximately parallel to the fibular and tibial shafts, with the other 2 gauges separated from the middle gauge by 45°. Before testing, an external microphone was placed near the test area to capture any audible pops, indicating an injury. A bone-mounted microphone (acoustic emission sensor) was also glued to the fibular midshaft to record the timing of subtle ligament injuries.

To measure the 3-dimensional kinematics of the ankle, sets of reflective, spherical markers were rigidly fixed to the tibia and calcaneus to track the kinematics of each bone during testing (Figure 1B). For each marker set, 4 reflective markers were rigidly attached to a plate, which was then attached to the bone by 2 wood screws each passing through an aluminum standoff. A multicamera, optoelectronic motion capture system (T-Series [hardware] and Nexus 2.2 [software]; Vicon) was used to measure the 3-dimensional motion of each marker in space during testing. The motions of the underlying tibia and calcaneus were then calculated from the measured marker-set motions via rigid-body transformation analysis (using CT scans of the instrumented specimen to document the locations of the marker sets relative to the bones).<sup>27</sup> External rotation of the foot relative to the leg was defined as rotation of the calcaneus about the long axis of the tibia.

### Testing Apparatus

Specimens were tested in a biaxial testing machine (Axial-Torsion Servohydraulic Fatigue Testing System and FastTrack 8800 Materials Test Control System; Instron). The potting cup at the proximal tibia was rigidly attached

to the Instron piston head (Figures 2 and 3) through a 6-axis load cell (Model 3868TF; Denton ATD). The Instron machine imparted the desired preload along the global Z-axis (defined as approximately the long axis of the tibia) and effective gross external rotation by rotating the tibia internally about the global Z-axis. Neutral ankle flexion was defined nominally in which a right angle was formed in the sagittal plane between the distal end of the first phalanx, approximate calcaneus centroid, and long axis of the tibia.<sup>16</sup>

Two sets of calcaneus boundary conditions were used for testing specimens. In the first (runs 1-3), a mount, assembled with acetal homopolymer resin and polyvinyl chloride and reinforced with machine screws, was placed around the calcaneus, constraining the calcaneus from rotating and translating relative to other ankle bones. A bidirectional linear rail system was rigidly attached to a gimbal system, which locked the foot in a neutral position (Figure 2). The calcaneus mount was rigidly fixed to the gimbal system, thus permitting foot translation in the global X (anterior-posterior) and Y (medial-lateral) directions and allowing the axis of external rotation to adjust to the natural axis of rotation in the lower limb.<sup>16</sup> The tibia internally rotated over the fixed calcaneus as it was free to translate, thus imparting external rotation. Boundary conditions consisted of 1 force ( $F_Z$  preload) and 3 moments ( $M_X$  reaction at calcaneus,  $M_Y$  reaction at calcaneus,  $M_Z$  input rotation torque) (Figure 2).

The second set of boundary conditions (runs 4-9) was designed to allow the foot and calcaneus to undergo natural inversion/eversion motion during the applied external rotation while keeping the foot supported by a pair of flat plates underneath (Figure 2). Lateral, opposing support blocks were placed to engage the heel and forefoot to apply external rotation: one block was placed lateral to the calcaneus, and one block was placed medial to the first metatarsal head to restrain the foot while the leg was internally rotated. These blocks acted as a substitute for feet constrained in a cleat on the football field, where the cleat is planted in the turf and the tibia internally rotates over the

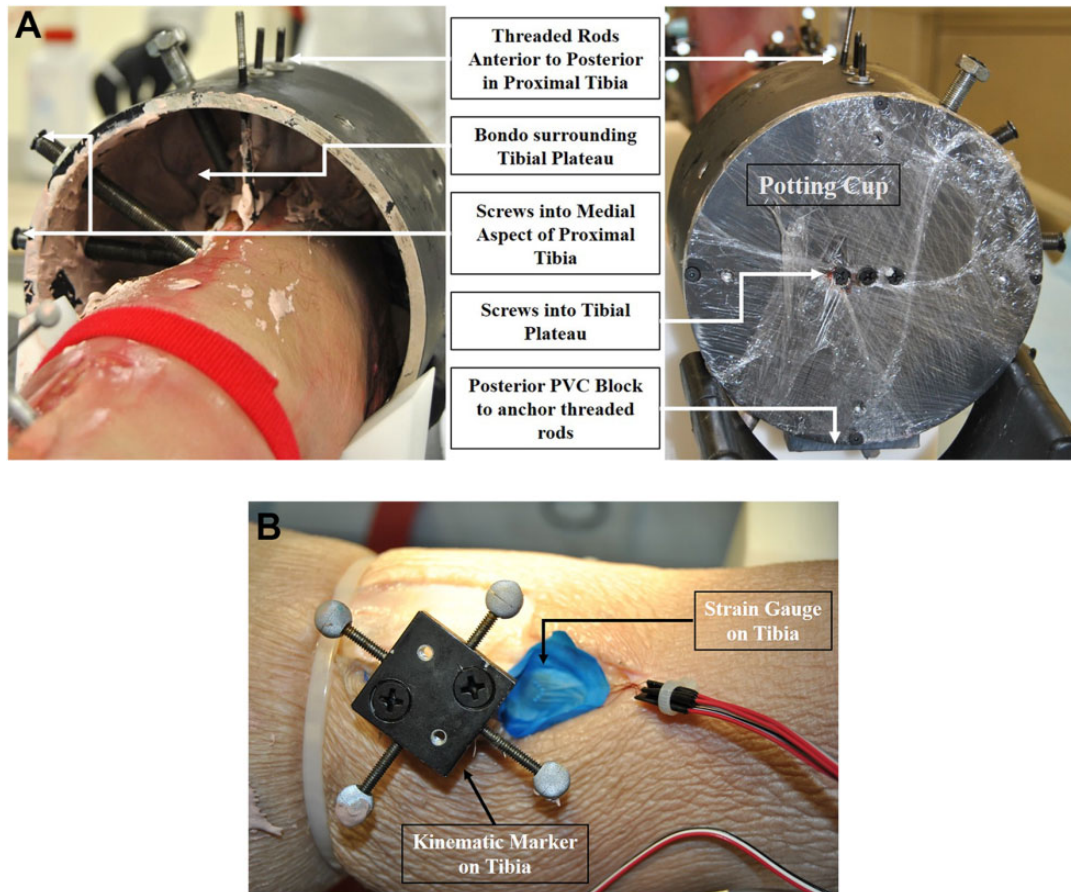


**Figure 1.** Specimen preparation photographs of a left leg showing (A) the tibial potting method and (B) kinematic marker placement and strain gauge attachment.

constrained foot.<sup>30</sup> To minimize binding, all surfaces in contact with the foot were lubricated (Tri-Flow Superior Teflon Chain Lube; Sherwin-Williams). The neutral initial foot position was maintained by orienting the plantar support plates parallel in the transverse (X-Y) plane. The arch of the foot was allowed to flatten during the preload, and the foot was allowed to translate in the anterior-posterior ( $\pm X$ ) direction during testing. Load cells (Models 6085 and 7414; Humanetics Innovative Solutions) were placed under the forefoot and hindfoot plates to capture reaction forces under both portions of the foot. Boundary conditions consisted of 3 forces ( $F_Z$  preload,  $F_Y$  reaction at first metatarsal head,  $F_Y$  reaction at calcaneus) and 3 moments ( $M_X$  reaction at forefoot and hindfoot,  $M_Y$  reaction at forefoot and hindfoot,  $M_Z$  input rotation torque) (Figure 2).

Boundary conditions for the plantar flexed and dorsiflexed tests (runs 10-17) (Figure 3) were similar to those in runs 4 to 9. To impart the desired degrees of ankle flexion, a wedge was rigidly fixed to the plantar foot plates: 15° was used for dorsiflexion and 30° for plantar flexion. To prevent the specimens from slipping down the inclined plates under the preload, a block was placed anterior to the toes in plantar flexion and posterior to the calcaneus in dorsiflexion. This restrained anterior-posterior foot translation; however, the natural axis of rotation of the tibia

was still able to adjust throughout the rotation cycle. All surfaces in contact with the foot were lubricated. Specimens were all tested in a flatfoot orientation such that the forefoot and hindfoot were aligned using the first metatarsal head and calcaneus blocks; no specimens were observed to exhibit hallux valgus or varus, or similar, foot orientations.

### Loading Protocol

Before testing, specimens were preconditioned by manually rotating the feet within physiological ranges of motion for ankle external-internal rotation, eversion-inversion, and dorsiflexion-plantar flexion.<sup>22,26</sup> For testing, all specimens were subjected to a compressive preload ( $F_Z$ ) targeting 2 kN (Table 1) through the tibia along the global Z-axis, chosen to simulate weightbearing during typical play situations.<sup>31,32</sup> This compressive preload was applied via the linear actuator of the Instron test machine. For all test runs, the Instron rotary actuator applied external rotation in a half-sine waveform. Rotation frequency was 0.05 Hz (18 deg/s) for run 1 and 0.025 Hz (9 deg/s) for all subsequent runs. Rotation magnitudes were varied, as we sought to find a magnitude that would consistently result in an injury (Table 1). Although rotation rates are less than those seen

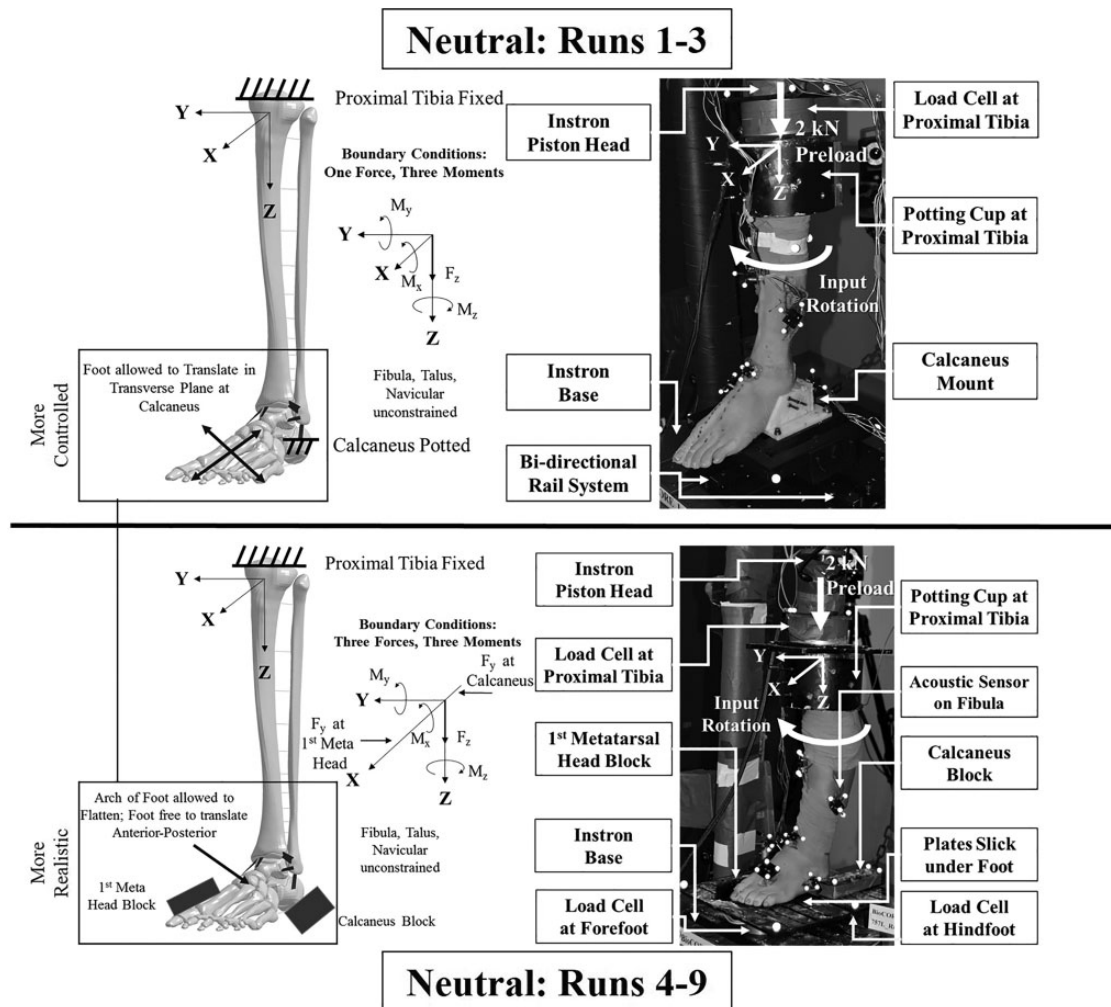


**Figure 2.** For runs 1 to 9, specimen test apparatus with pertinent fixture parts and instrumentation labeled and test apparatus schematic with boundary conditions identified in all neutral tests in runs 1 to 3 (top) with the calcaneus in a fixed orientation and runs 4 to 9 (bottom) with the calcaneus free to invert/evert.

clinically or on the playing field, low rotation rates were chosen to limit inertial effects and to be within physiological ranges.<sup>15,32</sup> The rotation rate was decreased after run 1 to limit binding in the test fixture for subsequent tests.

Kinetic and audio information was captured during testing for all specimens (Table 2). Load cells measured forces and moments at the proximal tibia, hindfoot, and forefoot. Strain gauges on the tibia and fibula were used to measure strain changes. An external microphone was placed next to the test area to capture audible pops, indicating an injury with high-energy release. A bone-mounted microphone (acoustic emission sensor) was also affixed to the fibula in an effort to record the timing of more subtle ligament injuries. Although not shown in Table 2, the instrumentation for runs 10 to 17 was the same as that used for runs 7 to 9.

**Clinical Evaluation**

After test completion, posttest radiographs and CT scans were obtained, in a nonloaded neutral ankle posture, to

document bony trauma. External rotation stress radiographs were not obtained on the specimens after testing. Two board-certified orthopaedic surgeons with fellowship training in sports medicine (R.B.A., M.T.C.) dissected all specimens to document injuries. Necropsies began at the proximal tibia and fibula and moved distally. Tissue was carefully removed to expose anatomic structures, namely, syndesmotic ligaments (ATiFL, PTiFL, and IOM), then medial ligaments (superficial deltoid [eg, anterior tibiotalar and tibionavicular ligaments] and deep deltoid [eg, 2 components branching from the tibia to the talus and to the calcaneus]),<sup>7,11</sup> and finally lateral ligaments (ATaFL, CFL, and PTaFL).<sup>7,11</sup>

**Determination of Injury Event Sequence**

After posttest necropsies, injury event sequences were determined for all runs. A group of biomechanical engineers, with consultation from orthopaedic surgeons, identified features of interest in the mechanical response (eg, moments/forces, strain, and audio) as possible injury

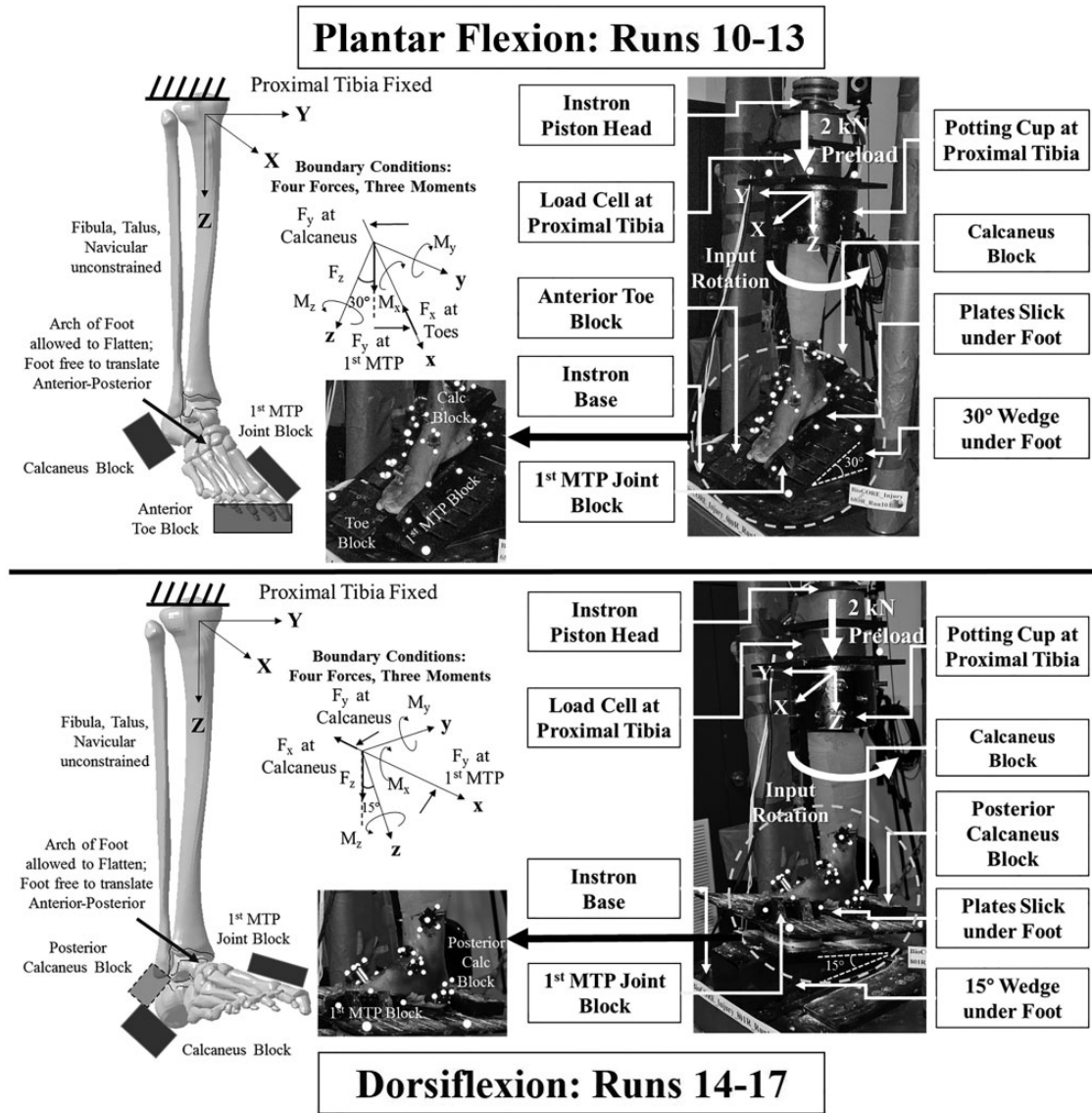


**Figure 3.** For runs 10 to 17, specimen test apparatus with pertinent fixture parts and instrumentation labeled and test apparatus schematic with boundary conditions identified in both the plantar flexion (top) and dorsiflexion (bottom) tests.

events.<sup>15</sup> Large changes in the mechanical response, especially in the moment about the global Z-axis, were typically attributed to bone fractures and failure of large ligaments (eg, deep deltoid and ATiFL). Small changes in the mechanical response were attributed to failure of small ligaments (eg, superficial deltoid and ATaFL). Features of interest in the strain and audio results were also used to identify potential injury events during the tests and to attribute to likely injury locations. For example, significant changes in strain on the tibia indicated injuries to the medial and syndesmotic ankle ligaments, whereas changes in strain on the fibula indicated injuries to the lateral and syndesmotic ankle ligaments. Understanding the strength and stoutness of certain ligaments, for example, the deep deltoid relative to the CFL or ATiFL relative to the superficial deltoid or IOM relative to the ATaFL,<sup>11,34</sup> helped further

distinguish injury events. A stronger ligament injury was indicated in conjunction with a larger drop in magnitude of force and moment response during testing. Combining this anatomic understanding with dissection results and study of mechanical response data, we were able to match diagnosed injuries with data events during each test. Cases in which specific injuries could not be reliably located in time, for example, those involving small ligaments or involving multiple injuries that occur nearly concurrently, are identified in Appendix Tables A1 to A4.

**RESULTS**

For each test, kinetic data for tibial and fibular strains and moments ( $M_z$  from the tibial load cell) were plotted against

TABLE 2  
Instrumentation Summary for All Neutral Tests

Instrumentation <sup>a</sup>	Run 1, Specimen 696R	Run 2, Specimen 680L	Run 3, Specimen 682L	Run 4, Specimen 615L	Run 5, Specimen 794L	Run 6, Specimen 801L	Run 7, Specimen 612L	Run 8, Specimen 752L	Run 9, Specimen 757L
Tibial load cells									
Force-x,y,z	X	X	X	X	X	X	X	X	X
Moment-x,y,z	X	X	X	X	X	X	X	X	X
Hindfoot load cells									
Force-x,y,z				X	X	X	X	X	X
Moment-x,y,z							X	X	X
Forefoot load cells									
Force-x,y,z				X	X	X	X	X	X
Moment-x,y,z				X	X	X	X	X	X
Strain gauges									
Tibia-1,2,3		X	X		X	X	X	X	X
Fibula-1,2,3		X	X		X	X	X	X	X
Acoustic emission				X	X		X	X	X
External microphone				X	X	X	X	X	X

<sup>a</sup>Instrumentation included 6-axis (3 forces and 3 moments) and 3-axis (3 forces) load cells, triaxial rosette strain gauges, a bone-mounted microphone (acoustic emission sensor), and an external microphone.

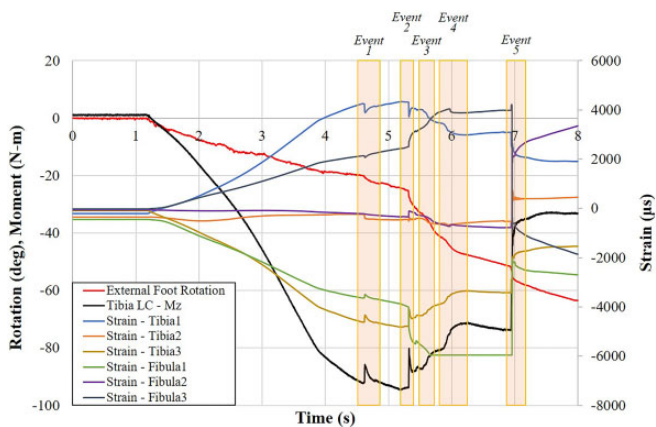


**Figure 4.** Representative plot of moment, strain, and external rotation data for specimen 794L in run 5 versus time with injury events identified. “Tibia LC” indicates the load cell attached to the proximal tibia.

time, with external rotation included for comparison. Separate plots were generated for moment, external microphone, and bone-mounted microphone data traces plotted against time, again with external rotation included for comparison. Examples of these data plots are shown for neutral (run 5, specimen 794L) (Figures 4 and 5).

The Appendix contains the complete clinical diagnoses from the necropsies (Appendix Tables A1-A4). The Appendix further contains the complete sequence of injuries for all tests. Figure 6 illustrates typical injury results for each of the 4 test conditions using 1 test from each condition.

As an example of the review process, the injuries diagnosed for run 5 included ligament failure of the superficial and deep deltoids, ATiFL, and IOM and a fibular fracture

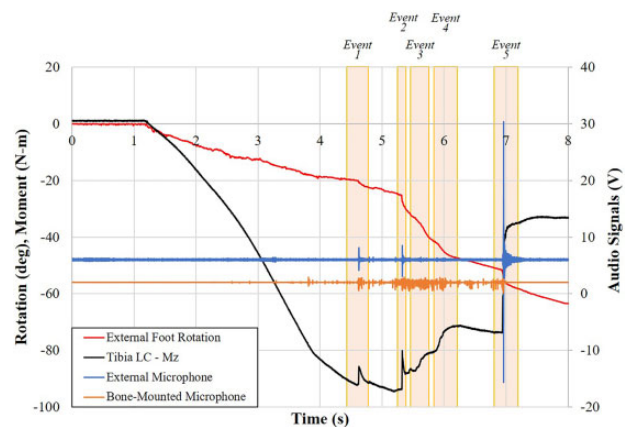


**Figure 5.** Plot of moment, external microphone, bone-mounted microphone (acoustic emission), and external rotation data for specimen 794L in run 5 versus time with injury events identified.

(Figure 7). Event 2 was attributed to failure in the deep deltoid, evidenced by the sudden, large decrease in moment combined with the sudden drop in tibial strain (Figure 4) but increase in fibular strain. Events 3 and 4 were attributed to progressive failure from distal to proximal of the ATiFL and IOM, respectively, evidenced by the gradual decrease in moment, despite increasing external rotation of the foot and perturbations in fibular strain. The largest change in moment occurred in event 5. This was attributed to a fracture of the fibula, also evidenced by corresponding strain and audio signals (Figures 4 and 5). The posttest dissection indicated that the fibular fracture occurred artifactually through the screw holes of the instrumentation (Figure 7). By process of elimination and supported by larger changes in tibial strain than in fibular strain,

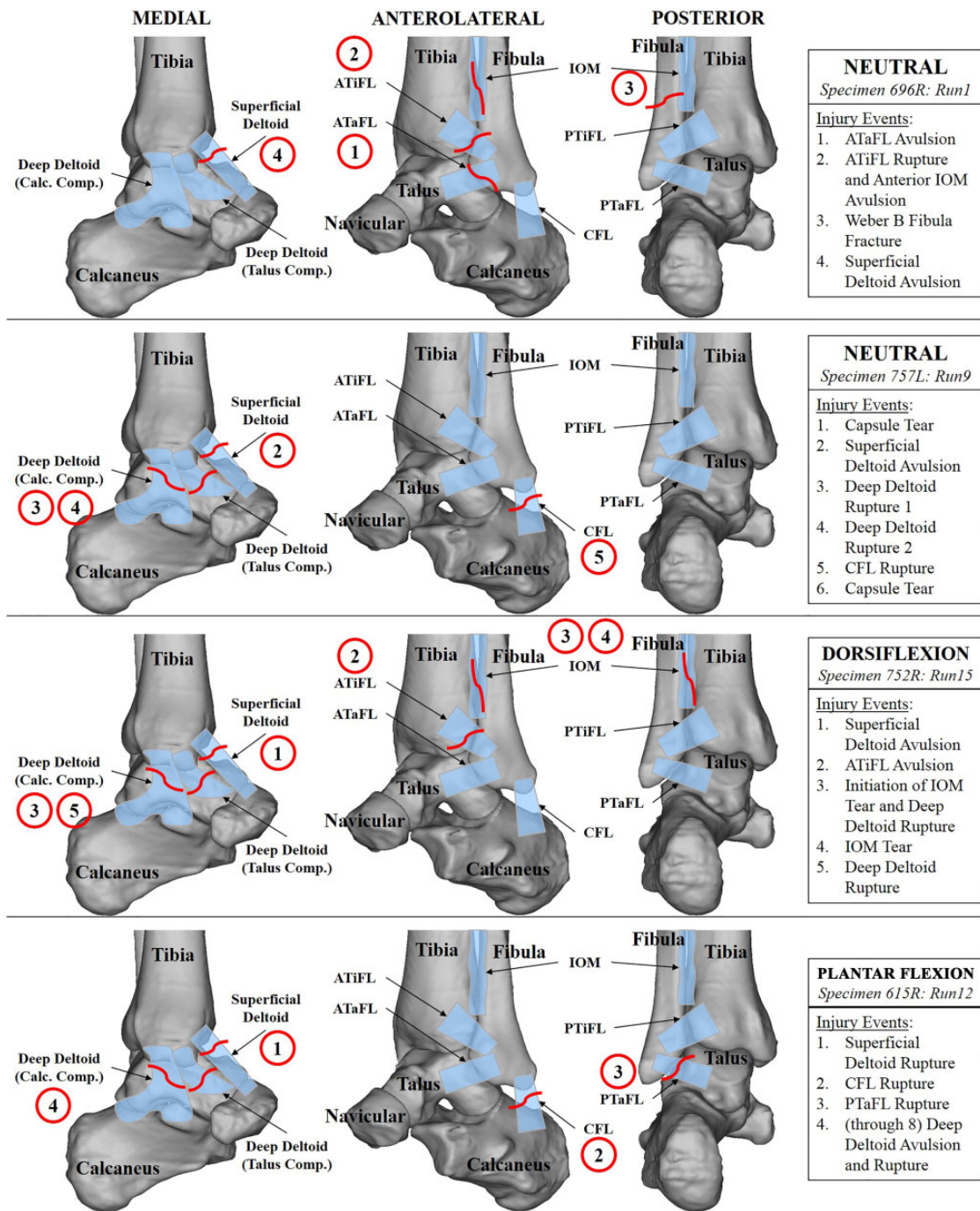


**Figure 6.** Illustrations of a representative injury event sequence for a neutral test with the calcaneus in a fixed orientation (specimen 696R, run 1), a neutral test with the calcaneus free to invert/everte (specimen 757L, run 9), a test with initial dorsiflexion (specimen 752R, run 15), and a test with initial plantar flexion (specimen 615R, run 12). Pertinent ligaments and bones are labeled in medial, anterolateral, and posterior views of the ankle. Injury events are detailed in the boxes on the right and highlighted in the illustrations with circles. ATaFL, anterior talofibular ligament; ATiFL, anterior tibiofibular ligament; CFL, calcaneofibular ligament; IOM, interosseous membrane; PTaFL, posterior talofibular ligament; PTiFL, posterior tibiofibular ligament.

event 1 was attributed to avulsion of the superficial deltoid from the tibia (Figures 4 and 7).

A syndesmotic injury was observed in 5 of the 9 initially neutral specimens, 0 of 4 for those initially plantar flexed,

and 4 of 4 for those initially dorsiflexed (Table 3). A medial ankle injury to the deltoid ligament complex was also common: the superficial deltoid was injured in 9 of 9 neutral specimens and 3 of 4 specimens for both plantar flexion and



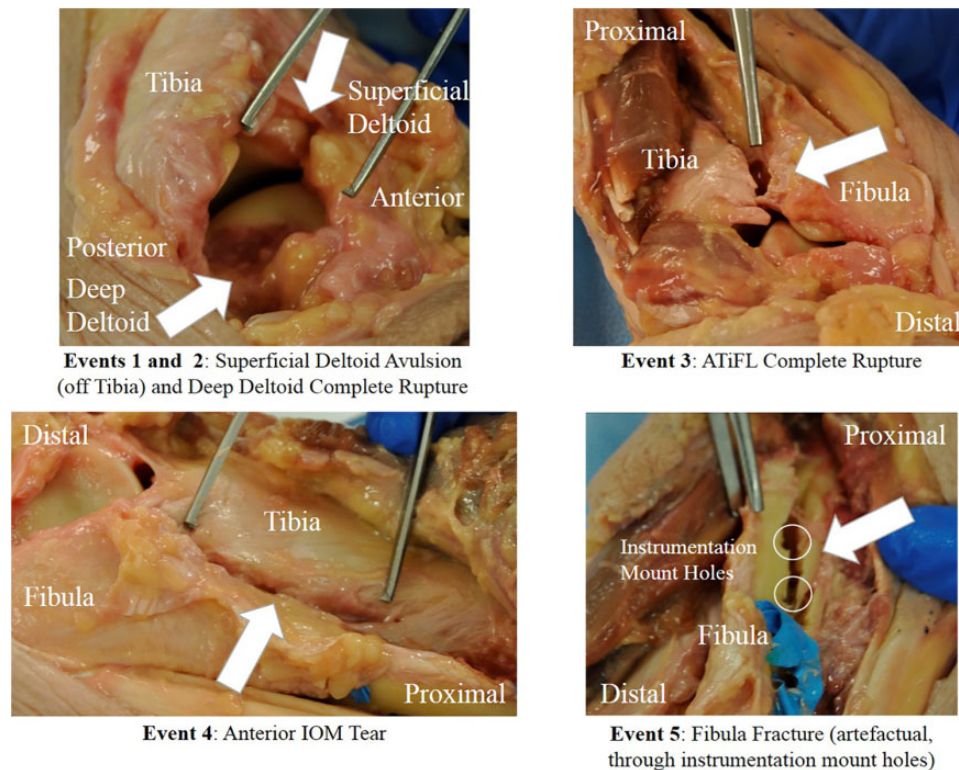


**Figure 7.** Posttest necropsy photographs for specimen 794L in run 5 indicating injuries attributed to an injury event. ATiFL, anterior tibiofibular ligament; IOM, interosseous membrane.

dorsiflexion. These injuries propagated to the deep deltoid for 5 of 9 neutral specimens, 3 of 4 specimens for plantar flexion, and 3 of 4 specimens for dorsiflexion. A lateral ankle injury was observed in 3 of 9 neutral specimens, 1 of 4 dorsiflexed specimens, and 3 of 4 plantar flexed specimens. Details of these injuries (including the severity of ligament injuries) are provided in Appendix Tables A1 to A4.

## DISCUSSION

This study sought to determine the sequence of injuries in ankle ligaments for lower limbs subjected to forced external rotation and to observe the sensitivity to initial ankle flexion posture. The results support the hypothesis that ankle flexion alters the incidence of syndesmotc injuries, ankle injury patterns, and the sequence of ankle injuries during forced external rotation. A syndesmotc injury occurred in over 50% of specimens initially in neutral, 0% in plantar flexion, and 100% in dorsiflexion (Table 3).

Previous studies conducted experiments to re-create syndesmotc ankle sprains in cadaveric limbs.<sup>18,19,31,32,35</sup> Several such experiments<sup>18,19,31,32</sup> rigidly connected the tibia to the fibula. Interactions between the tibia and fibula play an important role in the causation of syndesmotc ankle sprains, particularly through tibiofibular diastasis.<sup>14,29,35</sup> By rigidly coupling the tibia and fibula, the natural tibiofibular kinematic interaction is lost. Other experiments<sup>18,31,32,35</sup> prevented the foot from translating or the

arch of the foot from flattening, thus hindering natural interactions of all ankle and foot bones and subsequent ligament interaction during ankle rotation. In natural joint motion, external and internal rotations of the foot occur about a moving axis, which is determined by interactions between the tibia, fibula, talus, and calcaneus.<sup>4,25</sup> Restricting these to artificial, fixed axes of rotation has the potential to result in ankle bone kinematics and injury patterns that are not representative of what would occur naturally during hyperrotation. To address this, Mait et al<sup>16</sup> developed an experimental method designed to apply noninjurious external rotation to cadaveric limbs without artificially restricting the motion of the fibula or of the foot. This method was further investigated and implemented in the current study by testing specimens to failure (injury).

An injury to the medial ligaments has been proposed to be directly correlated to external rotation.<sup>3,8,29,33</sup> The results of this study support that hypothesis: deltoid injuries were generated in 15 of 17 specimens (Table 3 and Appendix Tables A1-A4). Wei et al<sup>31</sup> reported a similarly high incidence of injuries to the medial ligaments: 5 of 6 specimens tested in external rotation suffered deltoid injuries. Those authors further reported an absence of injuries to the PTiFL, which is also consistent with the results of the current study (Table 3). However, Wei et al<sup>31</sup> reported only 1 specimen with an injury to the ATiFL and no injuries to the IOM, whereas the current study found that 9 specimens suffered an injury to the ATiFL, with 5 of them suffering further

TABLE 3  
Injury Incidence Among All Initial Foot Postures<sup>a</sup>

Anatomic Structure	Plantar Flexion (n = 4)	Neutral (n = 9)	Dorsiflexion (n = 4)
ATiFL	0	5	4
IOM	0	3	2
PTiFL	0	0	0
Fibular fracture (Weber B or C)	0	1	1
Superficial deltoid	3	9	3
Deep deltoid	3	5	3
ATaFL	0	2	1
CFL	3	3	1
PTaFL	3	2	0
Fibular fracture (Weber A)	0	1	0
Tibial fracture (artefactual)	1	1	0
Fibular fracture (artefactual)	1	1	1

<sup>a</sup>Data are presented as No. Clinically significant ligament and bone fractures are noted beginning with the syndesmotoc region, then deltoid, and then lateral. The severity of ligament injuries varied among specimens: all severities (attenuations, avulsions, partial tears, and midsubstance ruptures) are grouped together. Artefactual (either through kinematic marker mounts or potting fixtures) tibial and fibular fractures are distinguished separately. ATaFL, anterior talofibular ligament; ATiFL, anterior tibiofibular ligament; CFL, calcaneofibular ligament; IOM, interosseous membrane; PTaFL, posterior talofibular ligament; PTiFL, posterior tibiofibular ligament.

injuries to the IOM (Table 3 and Appendix Tables A1-A4). Wei et al<sup>32</sup> aimed to re-create syndesmotoc ankle sprains under forced external rotation but observed mostly fibular fractures (4/10) and PTaFL fibular avulsions (4/10) as the main injuries, with only 1 specimen sustaining a medial ligament injury. In the external rotation experiments of Markolf et al,<sup>18</sup> 12 of 19 specimens experienced fibular fractures, 1 experienced a calcaneus fracture, 1 experienced a subtalar dislocation, and 5 experienced lateral ligament failure. Similarly, Michelson et al<sup>19</sup> generated a high occurrence of fibular fractures (15/30 specimens), a low occurrence of deltoid ligament injuries (4/30), and a low occurrence of ATiFL injuries (7/30). In contrast, in the current study, ATiFL injuries were more common than fibular fractures, occurring in 9 of 17 specimens tested compared with 7 of 17 experiencing fractures (Table 3).

These discrepancies in the generation of injuries could be attributed to differences in rotation magnitudes (ie, the current study rotated the tibia internally up to 90°), rotation rates, magnitudes of preload on the leg, and boundary conditions. The current study imposed rotation rates and preload magnitudes on the leg similar to previous studies investigating syndesmotoc ankle injuries<sup>30-32</sup>; therefore, the discrepancies in the generation of injuries could be mostly attributed to differences in applied boundary conditions. Markolf et al,<sup>18</sup> Michelson et al,<sup>19</sup> and Wei et al<sup>31,32</sup> all rigidly constrained the fibula to the tibia and either

rigidly fixed the foot or placed the foot in an unspecified, initially taped position. Rigidly constraining the tibia to the fibula artificially constrains the fibula in a manner that limits the natural occurrence of diastasis in the tibiofibular syndesmosis. When the ankle is forced into external rotation (under vertical preload), the talar dome wedges against the medial and lateral malleoli, forcing the syndesmosis to spread apart in diastasis. Concurrent with talar wedging in the intramalleolar mortise, with failure of anterior ankle ligaments (eg, ATaFL), posterior ligaments (eg, PTaFL) can act as a fulcrum about which the displaced fibula, caused by talar wedging, further rotates away from the tibia and compounds tibiofibular diastasis.

Under natural boundary conditions with the fibula only constrained by natural ligament attachments, this diastasis continues to build until the syndesmotoc ligaments and IOM rupture. When the fibula is unnaturally fixed to the tibia, however, any attempt to force the syndesmosis into diastasis also forces the fibula into bending (constrained by the attachment to the tibia). Because this fibular constraint limits diastasis, the artificial bending stress in the fibula builds faster than diastatic strain in the syndesmotoc ligaments. As a result, the failure mode changes from a syndesmotoc ligament injury (as would be expected in the field) to an artefactual fracture in the fibula. Clinically significant distal fibular fractures (ie, Weber classification) have been reported in athletes in association with syndesmotoc injuries<sup>14,23,33</sup> and were re-created in specimens tested in the current study (Appendix Tables A1-A4), differing from the artefactual fibular fractures observed in previous studies.<sup>18,19,31,32</sup> Thus, this highlights the importance of re-creating realistic boundary conditions, including allowing natural motion of the fibula, when studying injury mechanics in the ankle.

Another contributing factor to the differences in the generation of ligamentous versus bony injuries, between the current study and previous experiments is the difference in age and size of tested cadaveric specimens. The non-senescent, sizable cadaveric specimens tested in the current study (mean age at death, 47.0 years; mean height, 178.1 cm; mean weight, 94.4 kg) provided an important data source in replicating the mostly ligamentous syndesmotoc injury scenario seen among the athletic population. Prior studies used older participants; for example, age ranged from 49 to 85 years,<sup>18</sup> 60 to 80 years,<sup>19</sup> or 56 years, on average.<sup>31</sup> Bone deterioration with aging could have contributed to more bony fractures rather than soft tissue ruptures in those studies.

In addition to the boundary conditions on the tibia and fibula, care is also needed to ensure boundary conditions on the foot that are appropriate for studying ankle injuries. Although bone densitometry was not conducted to determine bone strength relative to observed deformations on specimens in this study, we contend that reduced constraint of the foot permits prefailure ligamentous leg and foot deformations (eg, tolerable tibiofibular diastasis and arch flattening) as well as foot translation. Each of these natural responses of the lower extremity is necessary to accurately re-create syndesmotoc ankle sprains.<sup>14,33</sup> The current study used 2 sets of boundary conditions: one with

a more controlled boundary condition in which the calcaneus was fixed in a defined orientation but allowed to translate freely in the anterior-posterior and lateral directions, and the other with a more realistic boundary condition in which the calcaneus was allowed to invert/evert freely and the foot allowed to flatten (under preload) against a support plate. Previous experiments constrained the tibia and fibula together and rotated these coupled bones over a rigid foot.<sup>18,19,32</sup> Others permitted fibular motion over a fixed foot<sup>35</sup> or constrained the foot with athletic tape,<sup>31</sup> thus creating an artificially restrictive boundary condition at the foot. Allowing natural fibular motion and foot translation affects bony kinematics and ligament recruitment in the ankle during foot rotation,<sup>15</sup> likely affecting resulting injury patterns and propagation sequences.

This is the first study, to our knowledge, to report full injury diagnoses and injury event sequences in external rotation experiments. Previous experiments<sup>18,19,31,32</sup> simply reported documented injuries, often limited to one observed injury, but did not report a sequence of injuries and propagation throughout the tests. Markolf et al<sup>18</sup> reported ligament tears during testing after fibular fractures occurred as more applied torque was resisted postfracture. However, only the injuries at proposed failure times were documented. Wei et al<sup>31</sup> and Michelson et al<sup>19</sup> plotted measured torque against applied external rotation and indicated "failure" by a single drop in torque during the loading phase. However, the current study found that multiple injuries happen throughout the entire rotation loading phase, often without or before a catastrophic drop in moment. Ligaments failed both before and after fractures of the tibia and fibula. Deltoid, ATiFL, and IOM failures often occurred concomitant with fibular fractures.

Previous studies have investigated the occurrence of syndesmotic injuries in varying ankle positions by combining external rotation with initially inverted ankles in dorsiflexion/plantar flexion<sup>19</sup> and with everted ankles.<sup>31</sup> However, to our knowledge, this is the first study to report syndesmotic injuries in varying angles of initial ankle flexion alone combined with external rotation. A close investigation of the incidence of diagnosed injuries (see Table 3) and injury event sequences (Appendix Tables A1-A4) suggests that ankle flexion has an effect on the occurrence of syndesmotic injuries in external rotation. In neutral ankle flexion, a syndesmotic injury was observed in 5 of 9 specimens. However, when combining external rotation with initial dorsiflexion, a syndesmotic injury occurred in all specimens (4/4). When external rotation was combined with initial plantar flexion, a syndesmotic injury occurred in no specimens. This suggests that plantar flexion might be protective of the syndesmosis, such that plantar flexion shifts the stress induced in the ankle ligaments from hyperrotation of the foot and, in turn, the resultant injuries from the syndesmotic ligaments to other ankle ligaments (deltoid and lateral).<sup>24</sup>

To cause these catastrophic injuries in a laboratory environment, cadaveric specimens must be utilized, but cadaveric specimens of a large size and young age at death are scarce commodities. Although the specimens tested in the current study were of a mean age older and mean size smaller than

those treated for syndesmotic injuries clinically, this study's sample of specimens are the youngest and largest, on the whole, tested in the literature, to our knowledge. Further limitations of this study include multiple boundary conditions tested on neutral legs and the censoring of injury data points.<sup>12</sup> Specimens were tested in hyperrotation of the foot intentionally to cause injuries and were not offloaded at the first indication of an injury. This test method confounds data censoring, such that discrete injuries are not associated with a single data point<sup>12</sup>; instead, a sequence of injuries was ascertained in this study for each specimen tested. The small sample size for each flexion posture (see Table 1), combined with the confounded censored injury data,<sup>12</sup> did not lend itself to statistical significance testing on the injury results; thus, statistical testing was not performed for the current study. In an effort to limit inertial effects during testing, legs were rotated at a lower rate than those experienced by athletes on the field, and a sensitivity study of the rotation rate was not performed for the current study.

Unlike previous studies,<sup>18,19,31,32</sup> the current study reports a method, although subjective, for determining the sequence of syndesmotic injuries in which both ligamentous and bony injuries are documented, with consultation from board-certified orthopaedic surgeons on all diagnosed injuries. We pragmatically chose specimens that met anthropometric specifications<sup>17</sup> so that an efficient study could be conducted. These assumptions and limitations are somewhat mitigated by testing matched-pair, contralateral legs such that a more direct correlation of the sequence of injuries to initial ankle flexion posture can be determined, however, this study should not be considered comprehensive for the human population and instead be considered for the specific, targeted anthropometry of large, young male patients.

Determining the sequence of injuries under external rotation helps elucidate the possible injury combinations that may be associated with a syndesmotic injury scenario. As deltoid injuries were common (15/17 specimens) (see Table 3) across all of the loading scenarios tested, these results suggest that it may be pertinent to suspect deltoid injuries in any clinical situation in which a syndesmotic ankle injury is indicated. Under hyperrotation of the foot, a syndesmotic injury was observed in 5 of 9 specimens in a neutral ankle flexion posture and in 4 of 4 specimens in a dorsiflexed posture. However, when external rotation was combined with initial plantar flexion, a syndesmotic injury occurred in no specimens. These results suggest that ankle flexion posture influences injury patterns in the ankle caused by external rotation, namely, that plantar flexion might be protective of the syndesmosis. Although not observed in all specimens tested, a possible propagation sequence for syndesmotic ankle sprains was observed in some specimens. Injuries often began in the medial ligaments and then propagated to either the syndesmotic or lateral ligaments (depending on ankle flexion), with possible propagation to the IOM and fibula.

Further studies will be performed to determine the possible kinematic or kinetic tolerance of syndesmotic ankle sprains during forced external rotation across varying initial foot positions. The injury sequence information determined in this study will enlighten clinical classifications of syndesmotic injuries to improve future care, recovery, and prevention methods. A

current finite element model<sup>20,21</sup> will be validated with this injury sequence to refine injury prediction capabilities within that model, with the ultimate goal of informing future diagnostic capabilities and countermeasure designs for reducing the incidence of syndesmotank ankle sprains in the field.

## CONCLUSION

In the nonsenescent, large male cadaveric legs tested in this study, the incidence of distal tibiofibular syndesmotank injuries decreased when hyper-external rotation of the foot was combined with ankle plantar flexion and increased when combined with ankle dorsiflexion compared with neutral matched-pair ankles. The propagation of ankle injuries was not identical in the legs tested; however, a characteristic sequence initiated with injuries to the medial ligaments, particularly the superficial deltoid, followed by propagation to either the syndesmotank or lateral ligaments (depending on ankle flexion), and finally to the IOM or fibula. Ankle dorsiflexion propagated this injury sequence to the syndesmotank ligaments, but plantar flexion propagated the sequence to the lateral ligaments.

For clinical relevance, as detailed in the current study, superficial deltoid injuries may occur in any case of hyper-external rotation of the foot, no matter the ankle flexion posture. Furthermore, a syndesmotank ankle injury is often concomitant with a superficial deltoid injury. However, a deep deltoid injury can be concomitant with a syndesmotank injury or offload the syndesmosis altogether.

## ACKNOWLEDGMENT

The authors thank the Foot and Ankle Subcommittee of the National Football League for funding, supporting, and providing valuable input to this study. The authors also thank Dr Matthew B. Panzer, Dr Patrick O. Riley, and Kevin Kopp for assistance in experimental design and data collection and thank Sara B. Heltzel for assistance in specimen acquisition and preparation.

## REFERENCES

- Anderson RB, Hunt KF, McCormick JJ. Management of common sports-related injuries about the foot and ankle. *J Am Acad Orthop Surg*. 2010;18:546-556.
- Bloemers FW, Bakker FC. Acute ankle syndesmosis injury in athletes. *Eur J Trauma*. 2006;32:350-356.
- Boytim MJ, Fischer DA, Neumann L. Syndesmotank ankle sprains. *Am J Sports Med*. 1991;19:294-298.
- Funk JR. Ankle injury mechanisms: lessons learned from cadaveric studies. *Clin Anat*. 2011;24:350-361.
- Funk JR, Hall GW, Crandall JR, Pilkey WD. Linear and quasi-linear viscoelastic characterization of ankle ligaments. *J Biomech Eng*. 2000;122:15-22.
- Gerber JP, Williams GN, Scoville CR, Arciero RA, Taylor DC. Persistent disability associated with ankle sprains: a prospective examination of an athletic population. *Foot Ankle Int*. 1998;19:653-660.
- Golano P, Vega J, de Leeuw PAJ, et al. Anatomy of the ankle ligaments: a pictorial essay. *Knee Surg Sports Traumatol Arthrosc*. 2016;24:944-956.
- Guise ER. Rotational ligamentous injuries to the ankle in football. *Am J Sports Med*. 1976;4:1-6.
- Hopkinson WJ, St Pierre P, Ryan JB, Wheeler JH. Syndesmosis sprains of the ankle. *Foot Ankle*. 1990;10:325-330.
- Jones MH, Amendola A. Syndesmosis sprains of the ankle: a systematic review. *Clin Orthop Relat Res*. 2007;455:173-175.
- Kaumeier G, Malone T. Ankle injuries: anatomical and biomechanical considerations necessary for the development of an injury prevention program. *J Orthop Sports Phys Ther*. 1980;1:171-177.
- Kent RW, Funk JR. *Data Censoring and Parametric Distribution Assignment in the Development of Injury Risk Functions From Biomechanical Data. Technical Paper 2004-01-0317*. Warrendale, Pennsylvania: Society of Automotive Engineers; 2004.
- Leardini A, O'Connor JJ, Catani F, Giannini S. The role of the passive structures in the mobility and stability of the human ankle joint: a literature review. *Foot Ankle Int*. 2000;21:602-615.
- Lin CF, Gross MT, Weinhold P. Ankle syndesmosis injuries: anatomy, biomechanics, mechanism of injury, and clinical guidelines for diagnosis and intervention. *J Orthop Sports Phys Ther*. 2006;36:372-384.
- Mait A. *Syndesmotank Ankle Sprains in Large Males* [master's thesis]. Charlottesville: Department of Mechanical and Aerospace Engineering, University of Virginia; 2017.
- Mait AR, Mane A, Forman JL, Donlon JP, Nie B, Kent RW. Transient and long-time kinetic responses of the cadaveric leg during internal and external foot rotation. *J Biomech*. 2017;53:196-200.
- Manfred T. Here's the ideal body type for every sport. *Business Insider*. 2014. Available at: <http://www.businessinsider.com/average-height-weight-nfl-nba-players-2014-8>. Accessed September 13, 2016.
- Markolf KL, Schmalzried TP, Ferkel RD. Torsional strength of the ankle in vitro: the supination-external-rotation injury. *Clin Orthop Relat Res*. 1989;246:266-272.
- Michelson J, Solocoff D, Waldman B, Kendell K, Ahn U. Ankle fractures: the Lauge-Hansen classification revisited. *Clin Orthop Relat Res*. 1997;345:198-205.
- Nie B, Panzer MB, Mane A, et al. Determination of the in situ mechanical behavior of ankle ligaments. *J Mech Behav Biomed Mater*. 2017; 65:502-512.
- Nie B, Panzer MB, Mane A, et al. A framework for parametric modeling of ankle ligaments to determine the in situ response under gross foot motion. *Comput Methods Biomech Biomed Engin*. 2016;19: 1254-1265.
- Nigg BM, Skarvan G, Frank CB, Yeaton MR. Elongations and forces of ankle ligaments in a physiological range of motion. *Foot Ankle*. 1990;11:30-40.
- Norkus SA, Floyd RT. The anatomy and mechanisms of syndesmotank ankle sprains. *J Athl Train*. 2001;36:68-73.
- Ozeki S, Kitaoka H, Uchiyama E, Luo ZP, Kaufman K, An KN. Ankle ligament tensile forces at the end points of passive circumferential rotation motion of the ankle and subtalar joint complex. *Foot Ankle Int*. 2006;27:965-969.
- Rastegar J, Miller N, Barmada R. An apparatus for measuring the load-displacement and load-dependent kinematic characteristics of articulating joints: application to the human ankle joint. *J Biomech Eng*. 1980;102:208.
- Roaaas A, Andersson GBJ. Normal range of motion of the hip, knee and ankle joints in male subjects, 30-40 years of age. *Acta Orthop Scand*. 1982;53:205-208.
- Shaw G, Parent D, Purtsezov S, et al. Impact response of restrained PMHS in frontal sled tests: skeletal deformation patterns under seat belt loading. *Stapp Car Crash J*. 2009;53:1-48.
- Taylor DC, Englehardt DL, Bassett FH. Syndesmosis sprains of the ankle: the influence of heterotopic ossification. *Am J Sports Med*. 1992;20:146-150.
- Teramoto A, Kura H, Uchiyama E, Suzuki D, Yamashita T. Three-dimensional analysis of ankle instability after tibiofibular syndesmosis injuries: a biomechanical experimental study. *Am J Sports Med*. 2008; 36:348-352.
- Wei F, Meyer EG, Braman JE, Powell JW, Haut RC. Rotational stiffness of football shoes influences talus motion during external rotation of the foot. *J Biomech Eng*. 2012;134:041002.

31. Wei F, Post JM, Braman JE, Meyer EG, Powell JW, Haut RC. Eversion during external rotation of the human cadaver foot produces high ankle sprains. *J Orthop Res.* 2012;30:1423-1429.

32. Wei F, Villwock MR, Meyer EF, Powell JW, Haut RC. A biomechanical investigation of ankle injury under excessive external foot rotation in the human cadaver. *J Biomech Eng.* 2010;132:091001.

33. Williams GN, Jones MH, Amendola A. Syndesmotic ankle sprains in athletes. *Am J Sports Med.* 2007;35:1197-1207.

34. Wolfe MW, Uhl TL, Mattacola CG, McCluskey LC. Management of ankle sprains. *Am Fam Physician.* 2001;63:93-104.

35. Xenos JS, Hopkinson WJ, Mulligan ME, Olson EJ, Popovic NA. The tibiofibular syndesmosis: evaluation of the ligamentous structures, methods of fixation, and radiographic assessment. *J Bone Joint Surg Am.* 1995;77:847-856.

APPENDIX

TABLE A1  
Injury Event Sequence for Neutral Tests 1 to 3<sup>a</sup>

Syndesmotic Injury	Injury Description
Run 1, specimen 696R	
Event 1	ATaFL partial avulsion off fibula; lateral capsule rupture with avulsion off talus
Event 2	X ATiFL complete rupture; anterior IOM avulsion from tibia
Event 3	X Weber B fibular fracture
Event 4	Superficial deltoid ligament avulsion off tibia
Run 2, specimen 680L	
Event 1	Superficial deltoid ligament avulsion off tibia
Event 2	X Inferior ATiFL complete rupture with small avulsion off lateral malleolus
Run 3, specimen 682L	
Event 1	Initiation of superficial deltoid ligament avulsion
Event 2	Superficial deltoid ligament 2-piece avulsion off tibia
Event 3	ATaFL 2-piece avulsion off fibula
Event 4-7	Continued propagation of avulsions

<sup>a</sup>ATaFL, anterior talofibular ligament; ATiFL, anterior tibiofibular ligament; IOM, interosseous membrane.

TABLE A2  
Injury Event Sequence for Neutral Tests 4 to 9<sup>a</sup>

Syndesmotic Injury	Injury Description
Run 4, specimen 615L	
Event 1	CFL avulsion off fibula
Event 2	Either superficial deltoid ligament avulsion off tibia or PTaFL partial avulsion off fibula
Event 3	Either superficial deltoid ligament avulsion off tibia or PTaFL partial avulsion off fibula
Event 4	Deep deltoid ligament avulsion off calcaneus
Run 5, specimen 794L	
Event 1	Superficial deltoid ligament avulsion off tibia
Event 2	Deep deltoid ligament complete rupture
Event 3	X ATiFL complete rupture
Event 4	X 33-mm tear of anterior IOM
Event 5	Artefactual fibular fracture
Run 6, specimen 801L	
Event 1	Superficial deltoid ligament 2-piece avulsion off tibia
Event 2	Weber A fibular fracture
Run 7, specimen 612L	
Event 1	X Inferior ATiFL and ATiFL complete ruptures
Event 2	Anterolateral joint capsule and posterior capsule tears
Event 3	Superficial deltoid ligament sleeve avulsion off tibia
Event 4	X Distal IOM partial disruption
Event 5	X Weber C fibular fracture
Event 6	Talus component of deep deltoid ligament complete rupture
Event 7	Artefactual tibial fracture

(continued)

TABLE A2 (continued)

Syndesmotic Injury	Injury Description
Run 8, specimen 752L	
Event 1	Either superficial deltoid ligament avulsion off tibia or off talus
Event 2	X Inferior ATiFL avulsion off tibia
Event 3	Either superficial deltoid ligament avulsion off tibia or off talus
Event 4	Either partial rupture of calcaneus component or complete rupture of talus component of deep deltoid ligament
Event 5	Either partial rupture of calcaneus component or complete rupture of talus component of deep deltoid ligament
Event 6	PTaFL complete rupture
Event 7	CFL complete rupture
Run 9, specimen 757L	
Event 1	Either anterolateral joint capsule tear or posterior tibial sheath rupture
Event 2	Superficial deltoid ligament sleeve avulsion off tibia
Event 3	Either calcaneus or talus component of deep deltoid ligament complete rupture
Event 4	Either calcaneus or talus component of deep deltoid ligament complete rupture
Event 5	CFL complete rupture
Event 6	Either anterolateral joint capsule tear or posterior tibial sheath rupture

<sup>a</sup>ATiFL, anterior tibiofibular ligament; CFL, calcaneofibular ligament; IOM, interosseous membrane; PTaFL, posterior talofibular ligament.

TABLE A3  
Injury Event Sequence for Plantar Flexion Tests<sup>a</sup>

Syndesmotic Injury	Injury Description
Run 10, specimen 680R	
Event 1	CFL 90% rupture or superficial deltoid ligament sleeve avulsion off medial malleolus
Event 2	CFL 90% rupture or superficial deltoid ligament sleeve avulsion off medial malleolus
Event 3	Initiation of deep deltoid ligament rupture (talus or calcaneus component)
Event 4	Deep deltoid ligament rupture (talus or calcaneus component)
Event 5	Deep deltoid ligament rupture (talus or calcaneus component)
Event 6	PTaFL avulsion off fibula
Run 11, specimen 612R	
Event 1	CFL midsubstance rupture
Event 2	PTaFL partial rupture
Event 3	Tibial comminuted fracture
Event 4	Fibular comminuted fracture
Run 12, specimen 615R	
Event 1	Superficial deltoid ligament sleeve avulsion off medial malleolus
Event 2	CFL complete rupture (avulsed off fibula)
Event 3	PTaFL complete rupture (avulsed off fibula)
Event 4-8	Deep deltoid ligament avulsion of calcaneus component and midsubstance rupture of talus component
Run 13, specimen 794R	
Event 1	Superficial deltoid ligament sleeve avulsion off medial malleolus
Event 2	Deep deltoid ligament complete rupture (talus or calcaneus component)
Event 3	Deep deltoid ligament complete rupture (talus or calcaneus component)

<sup>a</sup>CFL, calcaneofibular ligament; PTaFL, posterior talofibular ligament.

TABLE A4  
Injury Event Sequences for Dorsiflexion Tests<sup>a</sup>

Syndesmotic Injury		Injury Description
Run 14, specimen 682R		
Event 1		Superficial deltoid ligament sleeve avulsion off medial malleolus
Event 2	X	ATiFL mild attenuation or initiation of deep deltoid ligament rupture (talus component)
Event 3	X	ATiFL mild attenuation or further propagation of deep deltoid ligament ruptures (talus component)
Event 4		CFL midsubstance rupture
Event 5		Deep deltoid ligament rupture (talus component)
Event 6		Further propagation of deltoid ligament ruptures (talus component)
Run 15, specimen 752R		
Event 1		Superficial deltoid ligament avulsion off medial malleolus
Event 2	X	ATiFL avulsion off anterolateral distal tibia
Event 3		Initiation of IOM tear or deep deltoid ligament rupture (talus or calcaneus component)
Event 4	X	Anterior IOM tear
Event 5		Propagation of deep deltoid ligament ruptures (talus or calcaneus component)
Run 16, specimen 757R		
Event 1	X	ATiFL complete rupture
Event 2		Fibular fracture
Event 3		ATaFL mild attenuation
Event 4	X	Anterior IOM tear
Run 17, specimen 801R		
Event 1		Superficial deltoid ligament sleeve avulsion off medial malleolus
Event 2		Initiation of deep deltoid ligament rupture (talus or calcaneus component)
Event 3	X	ATiFL complete rupture
Event 4		Propagation of deep deltoid ligament ruptures (talus or calcaneus component)
Event 5	X	Weber B fibular fracture

<sup>a</sup>ATaFL, anterior talofibular ligament; ATiFL, anterior tibiofibular ligament; CFL, calcaneofibular ligament; IOM, interosseous membrane.